AIAA Guidance, Navigation, and Control Conference and Exhibit
15 - 18 August 2005, San Francisco, California

AIAA 2005-6257

Development of an Aerodynamic Database for a Generic Hypersonic Air Vehicle

Shahriar Keshmiri and Richard Colgren
The University of Kansas, Lawrence, KS 66045

Maj Mirmirani
California State University, Los Angeles, CA 90032

An overview of the aerodynamic characteristics, along with the process for developing an aerodynamic database for the Generic Hypersonic Vehicle (GHV), is presented in this paper. The experimental investigation of the aerodynamic characteristics for the blunt body of the GHV has been used as the core of the simulation model. The gaps in the wind tunnel data have been filled using the best available CFD results. The CFD results are compared with the equivalent wind tunnel data for authenticity. The expressions for the aerodynamic forces and the aerodynamic coefficients acting on the GHV are developed. The aerodynamic database covers the range of flight Mach numbers, angles of attack, sideslip angles, and control surface deflections. The aerodynamic model is then used within the simulation of the GHV.

Nomenclature

alt.	=	altitude, ft
b	=	lateral-directional reference length, span, ft
c	=	longitudinal reference length, mean aerodynamic chord, ft
C_D	=	total drag coefficient, n. d.
C_{Da}	=	drag increment coefficient for basic vehicle, n. d.
$C_{D\text{-}\delta a}$	=	drag increment coefficient for right elevon, n. d.
$C_{D\text{-}\delta e}$	=	drag increment coefficient for left elevon, n. d.
$C_{D\text{-}\delta r}$	=	drag increment coefficient for rudder, n. d.
C_L	=	total lift coefficient for basic vehicle, n. d.
C_{La}	=	lift increment coefficient for basic vehicle, n. d.
$C_{L\text{-}\delta a}$	=	lift increment coefficient for right elevon, n. d.
$C_{L\text{-}\delta e}$	=	lift increment coefficient for left elevon, n. d.
$C_{L\text{-}\delta r}$	=	lift increment coefficient for rudder, n. d.
C_Y	=	total side force, n. d.
$C_{Y\beta}$	=	side force with sideslip derivative for basic vehicle, n. d.
$C_{Y\text{-}\delta a}$	=	side force increment coefficient for right elevon, n. d.
$C_{Y\text{-}\delta e}$	=	side force, increment coefficient for left elevon, n. d.
$C_{Y\text{-}\delta r}$	=	side force, increment coefficient for rudder, n. d.
C_l	=	total rolling moment coefficient, n. d.
$C_{l\beta}$	=	rolling moment with sideslip derivative for basic vehicle, n. d.
$C_{l\text{-}\delta e}$	=	rolling moment increment for right elevon, n. d.
$C_{l\text{-}\delta e}$	=	rolling moment increment for left elevon, n. d.
$C_{l\text{-}\delta r}$	=	rolling moment increment for rudder, n. d.
C_{lp}	=	rolling moment with roll rate dynamic derivative, n. d.
C_{lr}	=	rolling moment with yaw rate dynamic derivative, n. d.
C_m	=	total pitching moment coefficient, n. d.
C_{ma}	=	pitching moment increment coefficient for basic vehicle, n. d.

*Graduate Student, Department of Aerospace Engineering, 2120 Learned Hall, and AIAA Student Member.
†Associate Professor, Department of Aerospace Engineering, 2120D Learned Hall, and AIAA Associate Fellow.
‡Professor and Chair, College of Engineering, Computer Science, and Technology, California State University, Los Angeles, 5151 State University, AIAA Associate Fellow.

$C_{m\text{-}\delta e}$ = pitching moment increment coefficient for right elevon, n. d.
$C_{m\text{-}\delta e}$ = pitching moment increment coefficient for left elevon, n. d.
$C_{m\text{-}\delta r}$ = pitching moment increment coefficient for rudder, n. d.
C_{mq} = pitching moment pitch rate dynamic derivative, n. d.
C_n = total yawning moment coefficient, n. d.
$C_{n\beta}$ = yawing moment with sideslip derivative for basic vehicle, n. d.
$C_{n\text{-}\delta a}$ = yawing moment increment coefficient for right elevon, n. d.
$C_{n\text{-}\delta e}$ = yawing moment increment coefficient for left elevon, n. d.
$C_{n\text{-}\delta r}$ = yawing moment increment coefficient for rudder, n. d.
C_{np} = yawing moment roll rate dynamic derivative, n. d.
C_{nr} = yawing moment yaw rate dynamic derivative, n. d.
I_{sp} = engine specific impulse, sec.
α = angle of attack, deg.
β = sideslip angle, red.
ϕ = engine fuel ratio, n.d.
M = mach number, n.d.
q_0 = dynamic pressure
$S_{ref.}$ = reference area, theoretical wing area , ft^2
T = engine net thrust, lb
X, Y, Z = total aerodynamic forces (in body coordinate x, y, and z)
V = vehicle free stream velocity, ft/sec
$\dot{W}$ = fuel flow rate, lb/sec
W_0 = initial value of vehicle weight, lb
W_{con} = weight of fuel consume
$X_{cg.}$ = longitudinal distance from momentum reference to vehicle c.g., positive aft, ft
I_{XX}, I_{YY}, I_{ZZ} = roll, pitch, and yaw moments of inertia respectively, slg-ft^2
n.d. = nondimensional
c.g. = vehicle center of gravity
SSTO = Single-Stage-To-Orbit
DOF = degrees of freedom
{q} = the rotation quaternion the rotational tensor of body frame w.r.t. Earth frame
$\{Q^{BE}\}$ = the rotational tensor of body frame w.r.t. the Earth frame
$\{\Omega^{BE}\}$ = angular velocity quaternion of body frame w.r.t. the Earth frame
[E] = identity matrix
p = roll rate
q = pitch rate
r = yaw rate
psf = pound per square feet
A.O.A = angle of attack, deg.
PLA = pilot lever angle, (0% to 100%)
thr = throttle angle

I. Introduction

The objective of this paper is to present a wind tunnel and CFD-based Six Degrees of Freedom (DOF) model for a generic hypersonic vehicle (GHV). The GHV simulation is developed to support NASA funded conceptual design studies of hypersonic flight vehicles at the Multidisciplinary Flight Dynamics and Control Laboratory at the California State University, Los Angeles, and the Flight Research Laboratory at the University of Kansas. The aerodynamic characteristics of the vehicle were developed using CFD studies conducted at NASA Langley, Rockwell International [1], and California State University, Los Angeles [2]. These were blended with wind tunnel results for a similar configuration wind tunnel tested at NASA Langley [3]. These results were digitized and organized into more than 80 lookup tables for this simulation. In addition, analytical expressions implemented as up to fifth order polynomials are developed based on the minimum values of Sum of Squares due to Error (SSE). A multiple cycle engine model is developed to cover subsonic, supersonic, and hypersonic speed ranges. Both MATLAB and visual Fortran codes were developed for the implementation of the nonlinear simulation. Results from straight and level flight, ascending, and descent flight are presented.

II. Vehicle Description

The three-view drawing of the Generic Hypersonic Vehicle (GHV) is given in Figure 1. Deflections of the elevons are measured with respect to the hinge line, which is perpendicular to the fuselage centerline. A fuselage, centerline-mounted vertical tail has a full span rudder with its hinge line at 25 percent of the chord from the trailing edge. Deflections of the rudder are measured with respect to its hinge line. Positive deflections are tailing edge left. Small canards (65 A series airfoil) are deployed at subsonic speeds for improved longitudinal stability and control. A sizing analysis of the vehicle yielded an estimated full-scale gross weight of 300,000 lbs and overall fuselage length of 200 ft. The vehicle empty weight is estimated 140,000 lbs. The airfoil section of wing has a symmetric diamond shape. The equations of motion account for the time varying center of mass, center of gravity, and moments of inertia as experienced during flight. It is assumed that c.g moves only along the body x-axis as fuel is consumed, vertical changes are not modeled. Fuel slosh is not considered, and the products of inertia are assumed negligible.

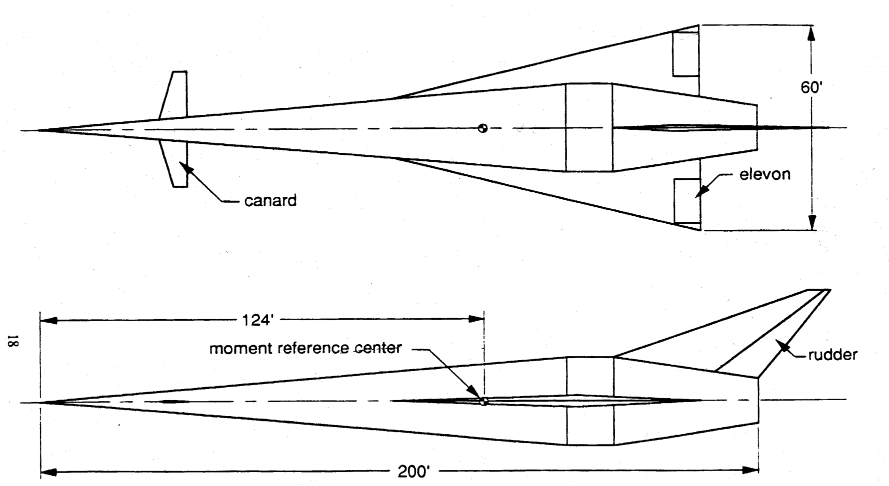

Figure 1: Three View of the Generic Hypersonic Vehicle

Table 1: Geometric Characteristics of the Generic Hypersonic Vehicle

Wing		
Reference area	ft^2	3603.00
Aspect ratio		1.00
Span	ft	60.00
Leading edge sweep angle	deg.	75.97
Trailing edge sweep angle	deg.	0.00
Mean aerodynamic chord	ft	80.00
Airfoil section	-	diamond

Airfoil thickness to chord ratio	%	4.00
Induced angle	deg.	0.00
Dihedral	deg.	0.00
Wing flap (elevon)		
Area each	ft^2	92.30
Chord (constant)	ft	7.22
Inboard section span location	ft	15
Outboard section span location	ft	27.78
Vertical tail, body centerline		
Exposed area	ft^2	645.70
Theoretical area	ft^2	1248.80
Span		32.48
Leading edge sweep angle	deg.	70.00
Trailing edge sweep angle	deg.	38.13
Airfoil section	-	diamond
Airfoil thickness to chord ratio	%	4.00
Rudder		
Area	ft^2	161.40
Span	ft	22.80
Chord of vertical tail chord ratio, percent	%	25.00
Canard		
Exposed area	ft^2	154.30
Theoretical area	ft^2	5.48
Span	ft	33.60
Leading edge sweep angle	deg.	16.00
Trailing edge sweep angle	deg.	0.00
Airfoil section	-	NACA 65A006
Induced angle	deg.	0.00
Dihedral	deg.	0.00
Axisymmetric fuselage		
Theoretical length	ft	200.00
Cone half angle	deg.	5.00
Cylinder radius (maximum)	ft	12.87
Cylinder length	ft	12.88
Boattail half angle	deg.	9.00
Boattail length	ft	40.00
Momentum reference center	ft	124.01

III. Aerodynamic Model

In order to develop a complete set of aerodynamic coefficients, experimental longitudinal and lateral-directional aerodynamics were obtained for the GHV by using six Langley wind tunnels. The data were obtained at Mach numbers from 0.6 t o 20.0; Reynolds numbers, based on model length, between 2.5 x l06 and 5.3 x l06, and angles of attack from -4° t o 20° [3]. The gaps in the wind tunnel data have been filled using the best available CFD results. The APAS code, which was developed by NASA Langley and Rockwell International Inc., and STARS, an all-new CFD solver developed for this project, are used. Due to the CFD code's airspeed modeling limitations in the transonic region, the CFD data was computed for the following Mach numbers: 0.3, 0.7, 2.5, 4.0, 6.0, 10.0, 15.0, and 24.0. The following angles of attack were used: 0.0°, 2.0°, 4.0°, 6.0°, 8.0°, 10.0°, and 12.0°. The coefficients were generated for a range of deflections of the right elevon, the left elevon, and the rudder for each Mach number and angle of attack combination. Each deflection was taken separately. Rudder deflections of -20.0°, -10.0°, 0.0°, 10.0°, and 20.0° were used for each surface. The lift, drag, and sideslip force, as well as the rolling, pitching, and yawing moment increment coefficients and derivatives are determined as functions of angle of attack and Mach number. The increment coefficients caused by the control surface deflections are determined as functions of angle of attack, surface deflection, and Mach number. They are added to the basic vehicle increments to form the total aerodynamic force and moment coefficients. Matlab code was developed and used to obtain coefficients of the polynomials describing the aerodynamic coefficients, (C_D, C_L, C_l, C_Y, C_m, and C_n).

IV. Aerodynamic Database

More than 80 look-up tables are developed based on the available wind tunnel and CFD results [1], [2], [3]. Generally, in control system design and specifically for the Simulink toolboxes, look-up table implementations are not suitable. For this specific reason a MATLAB program, FITTER, was written and applied to each look-up table to find the best analytical expression. The sum of squares due to error (SSE) measured the deviation of the look-up table values from the fitted values of the variables. A value closer to 0 indicates a better fit.

A. Lift Coefficient

The total lift coefficient is obtained as:
$C_L = C_{La} + C_{L\text{-}\delta a} + C_{L\text{-}\delta e}$ where, $C_L =$
$f(M, \alpha, \delta_a, \delta_e)$

<u>Subsonic</u>

C_{La} = - 5.2491e-004 + α. *1.5746e-002 + (α. *M).*6.0213e-003 - 3.4437e-004*α.^2
+ ((α. *M).^2).*1.4471E-04 - 5.1952E-05*α. ^3 + 3.4771E-05 *α.^4 + 2.7717E-03*M^4 - 2.3034E-06*α.^5

$C_{L\_\delta a}$ = - 5.119E-04 + 1.000E-03*α - 1.406E-04*(α*δa)+1.313E-03 *(α*M)
- 8.584E-04*(M*δa) + 8.879E-05*(α*M)* δa - 1.604E-04*M^2 - 3.477E-04*α^2
- 9.788E-05*(α*M)^2 - 1.703E-06*(M* δa)^2 + 2.532E-05*α^3 - 3.727E-05*δa ^3
+ 1.781E-07*δa ^2 + 7.912E-07*((α*M)* δa)^2 + 2.465E-08*(α*δa)^2 - 9.788E-05*(α*M)^2
- 5.942E-09 *((α*M)* δa)^3 - 7.377E-08*α^4 + 2.672E-08*δa ^4 - 1.610E-11*((α*M)* δa)^4
- 3.273E-08*α^5 + 7.624E-08*δa ^5 + 1.388E-13*((α*M)* δa)^5

$C_{L\_\delta e}$ = C_L_δa

<u>Supersonic</u>

C_{La} = + 1.9920e-01 + M* (2.3402e-01) + α.*(3.8202e-002) + (α.*M).* (-2.4626e-03)
+ (M.^2).* (-6.4872e-01) + (α.^2).* (-6.9523e-03) + ((α.*M.^2).^2).* (4.5735e-06)
+ (((α.^2).*M).^2).*(2.1241e-07) + ((α.*M).^2).*(-1.0521e-04) + (((α.^2).* M.^2).^2).*(-9.5825e-09)
+ (M.^3).*(3.9121e-01) + (α.^3).*(1.0295e-03) + (M.^4).*(-9.1356e-02) + (α.^4).*(-5.7398e-05)
+ (M.^5).*(7.4089e-03) + (α.^5).* (1.0934e-06)

$C_{L\_\delta a}$ = + (0)*1 + M.* (0) + α.* (0) + δa.* (0) + (α.* δa).* (-3.3093e-05) + (α.*M).* (0)
+ (M.* δa).* (-1.4287e-04) + ((α.*M).* δa).*(6.1071e-06) + (M.^2).*(0)
+ (α.^2).*(0) + (δa.^2).* (2.7242e-04) + (((α.*M).* δa).^2).* (-9.1890e-08) + ((α.* δa).^2).* (3.4060e-07)
+ ((α.*M).^2).*(-6.5093e-06) + ((M.* δa).^2).*(-6.3863e-06) + (M.^3).*(0) + (α.^3).*(1.4092e-04)
+ (δa.^3).*(3.8067e-06) + (((α.*M).* δa).^3).*(2.3165e-011)
+ (M.^4).*(-1.0680e-03) + (α.^4).*(-2.1893e-05) + (δa.^4).*(-3.7716e-07)
+ (((α.*M).* δa).^4).*(7.906e-014) + (M.^5).*(2.6056e-04) + (α.^5).*(9.2099e-07)
+ (δa.^5).*(-8.5345e-09) + (((α.*M).* δa).^5).*(-2.5698e-017)

$C_{L\_\delta e}$ = CL_δa

Hypersonic

C_{La} = - 8.19E-02 + M.* (4.70E-02) + α.*(1.86E-02) - (α.*M).* (4.73E-04)
- (M. ^2). * (9.19E-03) - (α.^2).*(1.52E-04) + ((α.*M).^2).* (5.99E-07)
+ (M.^3).*(7.74E-04) + (α.^3).*(4.08E-06) - (M.^4).*(2.93E-05)
- (α.^4).*(3.91E-07) + (M.^5).*(4.12E-07) + (α.^5).*(1.30E-08)

$C_{L\_\delta a}$ = - 1.45E-05 + α.*(1.01E-04) + M.*(7.10E-06) - δa.*(4.14E-04)
- (α.*δa).*(3.51E-06) + (α*M).* (4.70E-06) + (M.*δa).*(8.72E-06) - ((α.*M).* δa).*(1.70E-07)

$C_{L\_\delta e}$ = CL_δa

B. Drag Coefficient

The total drag coefficient is obtained as:
CD = C_{Da}+ $C_{D\text{-}\delta a}$ + $C_{D\text{-}\delta e}$ + $C_{D\text{-}\delta r}$ where, CD =
$f(M,\alpha,\delta_a,\delta_e,\delta_r)$

Subsonic

C_{Da} = + 1.1457e-02 + CL $_a$.* (-2.4645e-02) + M.*(0) + (CL $_a$.*M).*(4.9698e-02)
+ ((CL $_a$).^2).*(-1.9112e+00) + ((M).^2).*(0) + ((CL $_a$.*M).^2).*(3.5404e+00)
+ ((CL $_a$).^3).*(4.4334e+01) + ((M).^3).*(0) + ((CL $_a$.*M).^3).* (-7.0367e+01)
+ ((CL $_a$).^4).*(-2.3841e+02) + ((M).^4).*(0) + ((CL $_a$.*M).^4).*(4.1750e+02)
+ ((CL $_a$).^5).*(4.1734e+02) + ((M).^5).*(5.4910e-02) + ((CL $_a$.*M).^5).* (-7.9055e+02)

$C_{D\text{-}\delta a}$ = - 5.184e-04 + 1.100e-03*α + 3.38e-07*(α*δa) - 1.36e-03 *(α*M)
- 2.79e-04*(M*δa) - 1.53e-04 *(α*M)* δa +1.29e-03*(M^2) - 1.02e-04 *(α^2)
+ 9.39E-08*δa ^2 - 5.69E-07*((α*M)* δa)^2 + 4.14E-07 *(α*δa)^2 + 1.81E-04*(α*M)^2
- 1.68E-05*(M*δa)^2 - 1.84E-06*δa ^3 + 6.40E-08*α^4 + 5.76E-08*δa ^4
+ 5.71E-09*δa ^5 - 8.93E-15*((α*M)* δa)^5 - 7.58E-12*((α*M)* δa)^4 - 3.94E-10*((α*M)* δa)^3

$C_{D\text{-}\delta e}$ = $C_{D\_\delta a}$

$C_{D\text{-}\delta r}$ = + 2.47E-04 -1.93E-04 *α + 7.27E-05*(α*M) + 4.73E-05*M^2
+ 1.50E-05*α^2 + 5.03E-06*δr ^2 - 1.30E-07*((α*M)* δr)^2 - 3.50E-08*(α*δr)^2
- 1.68E-06*(α*M)^2 + 4.53E-06*(M*δr)^2 - 1.98E-11 * α^3 - 2.63E-08* α^4
+ 7.54E-09*δr ^4 + 3.12E-12*((α*M)* δr)^4

Supersonic

$C_{D\ a}$ = + (-8.2073e-02) + CL $_a$.* (-9.1273e-02) + M.*(2.1845e-01) + (CL $_a$.*M).*(3.2202e-02)
+ ((CL $_a$).^2).*(1.6325e+00) + ((M).^2).*(-1.3680e-01) + ((CL $_a$.*M).^2).*(5.7526e-02)

$+ ((C_{L\,a}).\text{^}3).*(-1.1575e+00) + ((M).\text{^}3).*(3.8791e-02) + ((C_{L\,a}.*M).\text{^}3).* (-2.402e-01)$
$+ ((C_{L\,a}).\text{^}4).*(-8.5306e+00) + ((M).\text{^}4).*(-5.2527e-03) + ((C_{L\,a}.*M).\text{^}4).*(3.5543e-01)$
$+ ((C_{L\,a}).\text{^}5).* (1.7259e+01) + ((M).\text{^}5).*(2.7435e-04) + ((C_{L\,a}.*M).\text{^}5).* (-1.4983e-01)$

$C_{D\text{-}\delta a}$ = + (0)*1 + M.* (0) + α.* (0) + δa.* (0)
+ (α.*δa).* (-3.6923e-05) + (α.*M).* (1.510e-05) + (M.* δa).*(1.3641e-07)
+ ((α.*M).* δa).* (5.1142e-06) + (M.^2).* (0) + (α.^2).* (0) + (δa.^2).* (1.2125e-05)
+ (((α.*M).* δa).^2).* (3.5662e-09) + ((α.*δa).^2).* (-1.3848e-08) + ((α.*M).^2).*(-4.7972e-07)
+ ((M.* δa).^2).*(-3.3763e-07) + (M.^3).*(0) + (α.^3).*(-4.6045e-08) + (δa.^3).*(3.9119e-08)
+ (((α.*M).* δa).^3).*(-9.7714e-013) + (M.^4).*(9.6475e-07) + (α.^4).*(1.5015e-08) + (δa.^4).*(4.5137e-09)
+ (((α.*M).* δa).^4).*(-6.6207e-016) + (M.^5).*(-3.2682e-07) + (α.^5).*(-3.5360e-010)
+ (δa.^5).*(-1.1538e-010) + (((α.*M).* δa).^5).*(4.1917e-019)

$C_{D\text{-}\delta e} = C_{D\text{-}\delta a}$

$C_{D\text{-}\delta r}$ = + (0)*1 + M.* (0) + α.* (0) + δr.* (0) + (α.*δr).* (2.6425e-021) + (α.*M).* (-9.8380e-06)
+ (M.* δr).* (1.8193e-020) + ((α.*M).* δr).* (1.0319e-021) + (M.^2).* (0)
+ (α.^2).* (0) + (δr.^2).* (8.7608e-06) + (((α.*M).* δr).^2).* (5.4045e-010) + ((α.*δr).^2).* (-2.8939e-08)
+ ((α.*M).^2).*(2.1842e-07) + ((M.* δr).^2).*(-2.9646e-07) + (M.^3).*(0)
+ (α.^3).*(-9.0067e-07) + (δr.^3).*(-8.8556e-022) + (((α.*M).* δr).^3).*(-5.2022e-027)
+ (M.^4).*(1.3388e-06) + (α.^4).*(1.6460e-07) + (δr.^4).*(4.6754e-010) + (((α.*M).* δr).^4).*(2.6560e-016)
+ (M.^5).*(-2.5185e-07) + (α.^5).*(-7.2766e-09) + (δr.^5).*(1.5611e-024) + (((α.*M).* δr).^5).*(5.4442e-033)

<u>Hypersonic</u>

C_{Da} = + 8.717E-02 - M.*(3.307E-02) + α.*(3.179E-03) - (α.*M).*(1.250E-04)
+ (M.^2).*(5.036E-03)- (α.^2).*(1.100E-03)
+ ((α.*M).^2).*(1.405E-07) - (M.^3).*(3.658E-04) + (α.^3).*(3.175E-04) + (M.^4).*(1.274E-05)
- (α.^4).*(2.985E-05) - (M.^5).*(1.705E-07) + (α.^5).*(9.766E-07)

$C_{D\text{-}\delta a}$ = + 1*(4.5548e-04) + α.*(2.5411e-05) + M.*(-1.1436e-04) + δa.*(-3.6417e-05)
+ ((α.*M).* δa).*(-5.3015e-07) + (α.^2).*(3.2187e-06) + (M.^2).*(3.0140e-06)
+ (δa.^2).*(6.9629e-06) + (((α.*M).* δa).^2).*(2.1026e-012)

$C_{D\text{-}\delta e} = C_{D\text{-}\delta a}$

$C_{D\text{-}\delta r}$ = + 7.50E-04 - α.*(2.2900E-05) - M.*(9.6900E-05) - δr.*(1.8300E-06)
+ ((α.*M).* δr).*(9.13E-09) + (α.^2).*(8.7600E-07) + (M.^2).*(2.7000E-06)
+ (δr.^2).*(1.9701E-06) - (((α.*M).* δr).^2)*.(1.7702E-11)

C. Side Force

The total side force coefficient is obtained as:
$C_Y = C_{Y\beta}\,\beta + C_{Y\text{-}\delta a} + C_{Y\text{-}\delta e} + C_{Y\text{-}\delta r}$ where β is in radians. $C_Y =$
$f(M,\alpha,\beta,d_e,d_a,d_r)$

<u>Subsonic</u>

$C_{Y\beta}$ = - 4.750E-01 - 5.000E-02*M

C_Y_δa = M.*(-1.845E-04) - (α.* δa).*(2.13E-07) + (α.*M).*(3.740E-05) + (M.* δa).*(1.990E-05)
+ ((α.*M).* δa).*(6.17E-08) + (α.^2).(3.39E-06) + (δa.^2).*(1.37E-07) - ((α.*M).^2)*(2.14E-06)
- (α.^3).*(1.11E-06)+ (δa.^3).*(- 3.40E-07) + (α.^4).*(1.09E-07)

+ (((α.*M).* δa).^2).*(3.53E-09) - ((α.* δa).^2).*(2.66E-09) + ((M.* δa).^2).*(3.92E-08)
+ (((α.*M).* δa).^3).*(5.42E-11) + (δa.^4).*(- 4.73E-10) + (((α.*M).* δa).^4).*(7.35E-14)
- (α.^5).*(3.45E-09) + (δa.^5).*(6.53E-10) - (((α.*M).* δa).^5)*(1.11E-15)

C_Y_δe = - (CY_δa)

C_Y_δr = + δr.* 2.440E-03

<u>Supersonic</u>

$C_{Y\beta}$ = + (0) + M* (0) + α.*(-1.1185e-02) + (α.*M).* (3.0432e-03) + (M.^2).*(-3.7586e-01)
+ (α.^2).*(3.4004e-03) + ((α.*M.^2).^2).* (-2.4047e-06) + (((α.^2).*M).^2).*(3.6104e-07)
+ ((α.*M).^2).*(-8.7176e-05) + (((α.^2).* M.^2).^2).*(-5.3622e-010) +(M.^3).*(0) + (α.^3).*(-5.8160e-04)
+ (M.^4).*(9.4289e-02) + (α.^4).*(4.4848e-05) + (M.^5).*(-1.8384e-02) + (α.^5).* (-1.3021e-06)

C_Y_δa = - 1.02E-06 - α.*(1.12E-07) + M.*(4.48E-07) + δa.*(2.27E-07) + ((α.*M).* δa).*(4.11E-09)
+ (α.^2).*(2.82E-09) – (M.^2).*(2.36E-08) + ((δa.) ^2).*(- 5.04E-08) + (((α.*M).* δa).^2).*(4.50E-14)

C_Y_δe = -(C_Y_δa)

C_Y_δr = + (0)*1 + M.* (0) + α.* (0) + δr.* (0) + (α.*δr).* (2.0067e-05) + (α.*M).* (0)
+ (M.* δr).* (-5.7185e-04) + ((α.*M).* δr).* (-1.5307e-05) + (M.^2).*(0) + (α.^2).* (0) + (δr.^2).* (1.9243e-019)
+ (((α.*M).* δr).^2).* (2.8011e-022) + ((α.*δr).^2).* (-2.0404e-021) + ((α.*M).^2).*(-1.2673e-020)
+ ((M.* δr).^2).*(-1.7950e-020) + (M.^3).*(0) + (α.^3).*(-9.9873e-019) + (δr.^3).*(3.2768e-05)
+ (((α.*M).* δr).^3).*(1.2674e-012) + (M.^4).*(-3.8438e-020) + (α.^4).*(1.9239e-019) + (δr.^4).*(7.7275e-023)
+ (((α.*M).* δr).^4).*(-3.2592e-029) + (M.^5).*(3.1048e-020) + (α.^5).*(-9.0794e-021) + (δr.^5).*(-6.5825e-08)
+ (((α.*M).* δr).^5).*(1.2684e-017)

<u>Hypersonic</u>

C_{Yb} = + (0) + * (-2.9253e-001) + α.*(2.8803e-003) + (α.*M).* (-2.8943e-004)
+ (M.^2).*(5.4822e-002) + (α.^2).* (7.3535e-004) + ((α.*M.^2).^2).* (-4.6490e-009)
+ (((α.^2).*M).^2).*(-2.0675e-008) + ((α.*M).^2).*(4.6205e-006) + (((α.^2).*M .^2).^2).*(2.6144e-011)
+ (M.^3).*(-4.3203e-003) + (α.^3).*(-3.7405e-004) + (M.^4).*(1.5495e-004)
+ (α.^4).*(2.8183e-005) + (M.^5).*(-2.0829e-006) + (α.^5).* (-5.2083e-007)

$C_{Y\_\delta e}$ = - 1.02E-06 - α.*(1.12E-07) + M.*(4.48E-07) + δa.*(2.27E-07)
+ ((α.*M.* δa).*(4.11E-09) + (α.^2).*(2.82E-09) - (M.^2)*(2.36E-08) - (δa.^2).*(5.04E-08)
+ (((α.*M.* δa).^2)*(4.50E-14)

C_Y_δe = -(C_Y_δa)

C_Y_δr = - 1.43E-18 + α.*(4.86E-20) + M.*(1.86E-19) + δr.*(3.84E-04)
- (α.*δr).*(1.17E-05) - (M.* δr).*(1.07E-05) + ((α.*M).* δr).*(2.60E-07)

D. Rolling Moment

The total rolling moment coefficient is:

$C_l = C_{l\beta}\,\beta + C_{l\text{-}}\delta_a + C_{l\text{-}}\delta_e + C_{l\text{-}}\delta_r + C_{lr}\left(\frac{rb}{2V}\right) + C_{lp}\left(\frac{pb}{2V}\right)$, where β is in radian, and the terms

$\left(\frac{pb}{2V}\right)$ and $\left(\frac{rb}{2V}\right)$ are the computed nondimensional roll and yaw rates so, $C_l = f(M, \alpha, \beta, \delta_e, \delta_a, \delta_r)$.

Subsonic

$C_{l\beta}$ = - 9.380E-02-M.*(1.250E-02)

$C_l.\delta_a$ = + 5.310E-05- α.*(5.272E-04) + (α.*δ_a).*(3.690E-05) + (α.*M).*(2.680E-05)
+ (M.* δ_a)*.(1.926E-04) - ((α.*M).* δ_a).*(8.500E-06) - (M.^2).*(4.097E-04)
+ (α.^2).*(1.258E-04) + (δ_a.^2).*(3.762E-06) - (((α.*M).* δ_a).^2).*(5.302E-08)
+ ((α.*M).^2).*(5.100E-06) + ((M.* δ_a).^2).*(2.100E-06) - (α.^3).*(8.700E-06) + (δ_a.^3).*(8.400E-06)
+ (((α.*M).* δ_a).^3).*(1.153E-09) - (((α.*δ_a).^2).*3.576E-08) + (α.^4).*(1.384E-08) - (δ_a.^4).*(1.137E-08)
+ ((((α.*M).* δ_a).^4).)*(1.011E-12) + (α.^5).*(1.381E-08) - (δ_a.^5).*(1.676E-08) - (((α.*M).* δ_a).^5).*(2.984E-14)

$C_l.\delta_e$ = -($C_l.\delta_a$)

$C_l.\delta_r$ =+ δ_r.*(7.000000E-04)

C_{lr} = + 2.625000E-01 + M.*(2.50E-02)

C_{lp} = - 1.337500E-01 - M.*(1.250000E-02)

Supersonic

$C_{l\beta}$ = + (0) + M* (0) + α.*(5.9211e-004) + (α.*M).*(-3.1579e-004) + (M.^2).*(-8.7296e-002)
+ (α.^2).*(-5.7398e-005) + ((α.*M.^2).^2).* (-1.1037e-006) + (((α.^2).*M).^2).*(-6.8068e-008)
+ ((α.*M).^2).*(2.0549e-005) + (((α.^2).* M.^2).^2).*(3.6561e-009) + (M.^3).*(0) + (α.^3).*(-2.8226e-016)
+ (M.^4).*(2.0334e-002) + (α.^4).*(1.9013e-007) + (M.^5).*(-3.7733e-003) + (α.^5).* (-9.6648e-019)

$C_l.\delta_a$ = + 3.570E-04 - 9.569E-05*α - 3.598E-05*M + 1.170E-04*δ_a + 2.794E-08*(α*M)* δ_a
+ 4.950E-06*α^2 + 1.411E-06*M^2 - 1.160E-06*δ_a ^2 - 4.641E-11*((α*M)* δ_a)^2

$C_l.\delta_e$ = -($C_l.\delta_a$)

$C_l.\delta_a$ =- 5.0103E-19 + 6.2723E-20*α + 2.3418E-20*M + 0.00011441*δ_r
- 2.6824E-06*(α*δ_r) -3.4201E-21*(α*M) - 3.5496E-06*(M*δ_r) + 5.5547E-08*(α*M)* δ_r

C_{lr} = + 3.82E-01 - 1.06E-01*M + 1.94E-03* α - 8.15E-05*(α*M) + 1.45E-02*M^2
- 9.76E-06*α^2 + 4.49E-08*(α*M)^2 - 1.02E-03*M^3 - 2.70E-07*α^3 + 3.56E-05*M^4
+ 3.19E-08*α^4 - 4.81E-07*M^5 -1.06E-09*α^5

C_{lp} = + (0) + M* (0) + α.*(-1.2668e-005) + (α.*M).* (1.7282e-005) + (M.^2).*(-1.0966e-001)
+ (α.^2).* (1.0751e-005) + ((α.*M.^2).^2).* (-1.0989e-006) + (((α.^2).*M).^2).*(6.1850e-009)
+ ((α.*M).^2).*(8.6481e-006) + (((α.^2).* M.^2).^2).*(-4.3707e-010) + (M.^3).*(0) + (α.^3).*(-1.1567e-005)
+ (M.^4).*(2.6725e-002) + (α.^4).*(1.5082e-006) + (M.^5).*(-5.0800e-003) + (α.^5).* (-6.1276e-008)

Hypersonic

$C_{l\beta}$ = - 1.402E-01 + M.*(3.326E-02) - α.*(7.590E-04) + (α.*M).*(8.596E-06) + (M.^2).*(- 3.794E-03)
+ (α.^2).*(2.354E-06) - ((α.*M).^2).*(1.044E-08) + (M.^3).*(2.219E-04) - (α.^3).*(8.964E-18)
- (M.^4).*(6.462E-06) + (α.^4).*(3.803E-19) + (M.^5).*(7.419E-08) - (α.^5).*(3.353E-21)

$C_{l\text{-}}\delta_a$ = + 3.570E-04 - α.*(9.569E-05) - M.*(3.598E-05) + δ_a.*(1.170E-04) + ((α.*M).* δ_a).*(2.794E-08)
+ (α.^2).*(4.950E-06) + (M.^2).*(1.411E-06) - (δ_a.^2).*(1.160E-06) - (((α.*M).* δ_a).^2)*(4.641E-11)

$C_{l\text{-}}\delta_e$ = -($C_{l\text{-}}\delta_a$)

$C_{l\text{-}}\delta_r$ = - 5.0103E-19 + α.*(6.2723E-20) + M.*(2.3418E-20) + δ_r.*(1.1441E-04)
- ((α.*δ_r).*(2.6824E-06) - ((α.*M).*(3.4201E-21) - (M.* δ_r)).*(3.5496E-06) + ((α.*M).* δ_r).*(5.5547E-08)

C_{lr} = + 3.82E-01 - M.*(1.06E-01) + α.*(1.94E-03) - ((α.*M).*(8.15E-05))
+ (M.^2).*(1.45E-02) - (α.^2).*(9.76E-06) + ((α.*M).^2).*(4.49E-08) - (M.^3).*(1.02E-03*) - (α.^3).*(2.70E-07)
+ (M.^4).*(3.56E-05) + (α.^4).*(3.19E-08) - (M.^5).*(4.81E-07) - (α.^5).*(1.06E-09)

C_{lp} = - 2.99E-01 + M.*(7.47E-02) + α.*(1.38E-03) - (α.*M).*(8.78E-05)
- (M.^2).*(9.13E-03) - (α.^2).*(2.04E-04) - ((α.*M).^2).*(1.52E-07) + (M.^3).*(5.73E-04)
- (α.^3).*(3.86E-05*) - (M.^4).*(1.79E-05) + (α.^4).*(4.21E-06) + (M.^5).*(2.20E-07) - (α.^5).*(1.15E-07)

E. Pitching Moment

The total pitching moment coefficient is obtained as: $C_m = C_{ma} + C_{m\text{-}\delta a} + C_{m\text{-}\delta e} + C_{m\text{-}\delta r} +$

$C_{mq}\left(\frac{q\,c}{2\,V}\right)$, where $\left(\frac{q\,c}{2\,V}\right)$ is the computed non-dimensional pitch rate.

If the pitching moment about the c.g. is required then we have:

$$\overline{M}_{mrc} = \bar{q}\, c\, S_{ref.} C_m$$
$$\overline{M} = \overline{M}_{mrc} - x_{cg} Z$$
$$\text{where Z - axis force is given by}$$
$$Z = -\,D \sin\alpha - L \cos\alpha$$

<u>Subsonic</u>

C_{ma} = + (-1.8316e-03) + CL $_a$.* (-1.0306e-01) +M.*(0) + (CL $_a$.*M).*(-1.8335e-01)
+ ((CL $_a$).^2).*(-1.1839e+00) + ((M).^2).*(-2.8113e-03) + ((CL $_a$.*M).^2).*(-1.3362e+00)
+ ((CL $_a$).^3).*(9.0641e+00) + ((M).^3).*(0) + ((CL $_a$.*M).^3).* (2.6964e+01)
+ ((CL $_a$).^4).*(-6.3590e+01) + ((M).^4).*(0) + ((CL ^{a}.*M).^4).*(-8.0921e+01)
+ ((CL $_a$).^5).* (1.6885e+02)+ ((M).^5).*(0) + ((CL $_a$.*M).^5).* (-4.2209e+00)

$C_{m\_\delta a}$ = + 2.880E-04 - (α.*(5.3510E-04) + ((α.* δ_a).*(4.5500E-05) + (α.*M).*(3.3790E-04)
+ (M.* δ_a).*(6.665E-04) - ((α.*M).* δ_a).*(2.770E-05) - (M.^2).*(6.027E-04) + ((α.^2).*(92.660E-05)
- (δ_a.^2).*(1.600E-06) - ((α.*M).* δ_a).^2).*(1.000E-07) - ((α.*M).^2).(1.910E-05)
+ ((M.* δ_a).^2).*(2.300E-06*) + ((α.^3).*(1.300E-05) + (δ_a.^3).*(1.920E-05) + ((α.*M).* δ_a).^3).*(1.90E-09)
- ((α.^4).*(1.861200E-06) - (δ_a.^4).*(4.69E-10) + ((α.*M).* δ_a).^4).*(1.29E-12)
+ ((α.^5).*(7.29E-08) - (δ_a.^5).*(3.87E-08) - ((α.*M).* δ_a).^5).*(4.67E-14)

$C_{m}\_\delta_e$ = Cm_δ_a

$C_{m}\_\delta_r$ = - 1.841E-04 + (α.*(3.5E-06)) + M.*(2.762E-04) - δ_r.*(1.0E-07)
- (α.^2).*(4.0E-07) + (δ_r.^2).*(5.8E-06) + (((α.*M).* δ_r).^2).*(6.482E-09)

C_{mq} = - 1.0313 - M.*(3.1250E-01)

Supersonic

C_{ma} = + (-5.7643e-001) + M* (1.0553e+0) + CL $_a$.*(-3.7951e-01) + (CL a.*M).* (1.0483e-01)
+ (M.^2).* (-7.4344e-01) + (CL $_a$.^2).* (-1.5412e-01) + ((CL $_a$.*M.^2).^2).* (-2.1133e-03)
+ (((CL $_a$.^2).*M).^2).*(-1.7858e-01) + ((CL $_a$.*M).^2).*(5.7805e-002) + (((CL $_a$.^2).* M.^2).^2).*(-3.8875e-03)
+ (M.^3).*(2.5341e-01)+ (CL $_a$.^3).*(-4.9731e-01) + (M.^4).*(-4.1938e-02)
+ (CL $_a$.^4).*(7.1784e+00) + (M.^5).*(2.7017e-03) + (CL $_a$.^5).* (-1.0331e+01)

Cm_δ_a = - 5.67E-05 - α.*(6.59E-05) - M*(1.51E-06) + δ_a.*(2.89E-04)
+ (α.*δ_a).*(4.48E-06) - (α.*M).*(4.46E-06) - (M.* δ_a).*(5.87E-06) + ((α.*M).* δ_a).*(9.72E-08)

C_m_δ_e = Cm_δ_a

C_m_δ_r = α.*(- 2.79E-05*) - (α.^2).*(5.89E-08) + (M.^2).*(1.58E-03) + (α.^3).*(6.42E-08)
- (M.^3).*(6.69E-04) - (α.^4).*(2.10E-08) + (M.^4).*(1.05E-04) + (δ_r.^4).*(1.43E-07)
+ (α.^5).*(3.14E-09) - (M.^5).*(7.74E-06) - (δ_r.^5).*(4.77E-22) - (α.^6).*(2.18E-10)
+ (M.^6).*(2.70E-07) - (δ_r.^6).*(3.38E-10) + (α.^7).*(5.74E-12) - (M.^7).*(3.58E-09)
+ (δ_r.^7).*(2.63E-24)

C_{mq} = + (0) + M* (0) + α.*(-1.0828e-02) + (α.*M).* (4.2311e-03)
+ (M.^2).* (-6.1171e-01)+ (α.^2).*(4.6974e-03) + ((α.*M.^2).^2).* (-1.1593e-05)
+ (((α.^2).*M).^2).*(2.5378e-07) + ((α.*M).^2).*(-7.0964e-05)
+ (((α.^2).* M.^2).^2).*(4.1284e-08) + (M.^3).*(0) + (α.^3).*(-1.1414e-03)
+ (M.^4).*(1.5903e-01) + (α.^4).*(1.1176e-04) + (M.^5).*(-3.0665e-02) + (α.^5).* (-3.8123e-06)

Hypersonic

C_{ma} = - 2.192E-02 + M.*(7.739E-03) - α.*(2.260E-03) + (α.*M).*(1.808E-04)
- (M.^2).*(8.849E-04) + (α.^2).*(2.616E-04) - ((α.*M).^2).*(2.880E-07)
+ (M.^3).*(4.617E-05) - (α.^3).*(7.887E-05) - (M.^4).*(1.143E-06) + (α.^4).*(8.288E-06)
+ (M.^5).*(1.082E-08) - (α.^5).*(2.789E-07)

Cm_δ_a = - 5.67E-05 - α.*(6.59E-05) - M*(1.51E-06) + δ_a.*(2.89E-04)
+ (α.*δ_a).*(4.48E-06) - (α.*M).*(4.46E-06) - (M.* δ_a).*(5.87E-06) + ((α.*M).* δ_a).*(9.72E-08)

C_m_δ_e = Cm_δ_a

C_m_δ_r = α.*(- 2.79E-05*) - (α.^2).*(5.89E-08) + (M.^2).*(1.58E-03)+ (α.^3).*(6.42E-08)
- (M.^3).*(6.69E-04) - (α.^4).*(2.10E-08) + (M.^4).*(1.05E-04) + (δ_r.^4).*(1.43E-07)
+ (α.^5).*(3.14E-09) - (M.^5).*(7.74E-06) - (δ_r.^5).*(4.77E-22) - (α.^6).*(2.18E-10)
+ (M.^6).*(2.70E-07) - (δ_r.^6).*(3.38E-10) + (α.^7).*(5.74E-12) - (M.^7).*(3.58E-09)
+ (δ_r.^7).*(2.63E-24)

C_{mq} = - 1.36E+00 + M.*(3.86E-01) + α.*(7.85E-04) + (α.*M).*(1.40E-04)
- (M.^2).*(5.42E-02) + (α.^2).*(2.36E-03) - ((α.*M).^2).*(1.95E-06)
+ (M.^3).(3.80E-03) - (α.^3).*(1.48E-03) - (M.^4).*(1.30E-04) + (α.^4).*(1.69E-04)
+ (M.^5).(1.71E-06) - (α.^5).*(5.93E-06)

F. Yawing Moment

The total yawing moment coefficient is obtained as:

$C_n = C_{nB}\,\beta + C_{n\text{-}\delta a} + C_{n\text{-}\delta e} + C_{n\text{-}\delta r} +$

$C_{nr}\left(\frac{r\,b}{2\,V}\right) + \ldots \quad C_{np}\left(\frac{p\,b}{2\,V}\right)$ where β is in radians, and the terms $\left(\frac{p\,b}{2\,V}\right)$ and $\left(\frac{r\,b}{2\,V}\right)$ are the computed nondimensional roll and yaw rates.

$$C_n = f(M,\alpha,\beta,d_e,d_a,d_r)$$

$$\overline{N}_{mrc} = \overline{q}\,b\,S_{ref.}C_n$$

$$\overline{N} = \overline{N}_{mrc} + x_{cg}Y$$

Subsonic

C_{nB} = + 1.062E-01 + M.*(6.250E-02)

$C_{n\text{-}\delta a}$ = (α.*δ_a).*(-2.7000e-07) - (M.* δ_a).*(1.008E-05) + ((α.*M).* δ_a).*(3.564E-07)
+ (δ_a.^3).*(1.1000e-07) + (δ_a.^3).*(1.11E-07) - (((α.*M).* δ_a).^3).*(9.32E-12)
- (α.^4).*(1.9910e-021)+ (δ_a.^4).*(2.89E-25) + (((α.*M).* δ_a).^4).*(1.82E-28)
+ (α.^5).*(6.95E-23) - (δ_a.^5).*(2.2046e-010) + (((α.*M).* δ_a).^5).*(2.22E-16)

$C_{n\text{-}\delta e}$ = -($C_{n\text{-}\delta a}$)

$C_{n\text{-}\delta r}$ = δ_r.*(- 3.000E-03)

C_{np} = + 1.790E-01 + M*(2.000E-02)

C_{nr} = - 1.2787 - M*(1.375e-001)

Supersonic

C_{nB} = + (0) + M* (0) + α.*(-2.3745e-03)
+ (α.*M).* (8.5307e-04) + (M.^2).* (1.4474e-01) + (α.^2).* (5.3105e-04)
+ ((α.*M.^2).^2).* (-8.3462e-07) + (((α.^2).*M).^2).*(1.3335e-07) + ((α.*M).^2).*(-2.7081e-05)
+ (((α.^2).* M.^2).^2).*(-1.3450e-09) + (M.^3).*(0) + (α.^3).*(-4.1046e-05)
+ (M.^4).*(-3.9519e-02) + (α.^4).*(-1.5141e-06) + (M.^5).*(7.7646e-03) + (α.^5).* (1.7278e-07)

$C_{n\text{-}\delta a}$ = + 2.10E-04 + α.*(1.83E-05) - M.*(3.56E-05) - δ_a.*(1.30E-05)
- ((α.*M).* δ_a).*(8.93E-08) - (α.^2).*(6.39E-07) + (M.^2).*(8.16E-07) + (δ_a.^2).*(1.97E-06)
+ (((α.*M).* δ_a).^2).*(1.41E-11)

$C_{n\text{-}\delta e}$ = -($C_{n\text{-}\delta a}$)

$C_{n\text{-}\delta r}$ = + 2.85E-18 - α.*(3.59E-19) - M.*(1.26E-19) - δ_r.*(5.28E-04)
+ (α.*δ_r).*(1.39E-05)+ (α.*M).*(1.57E-20) + (M.* δ_r).*(1.65E-05) - ((v.*M).* δ_r).*(3.13E-07)

C_{np} = + (1.7000e-01) + α.* (-6.4056e-018) + M.*(1.1333e-02) + (α.*M).*(2.3467e-018)
+ ((α).^2).*(2.0917e-019) + ((M).^2).*(-5.3333e-03) + ((α.*M).^2).*(-5.0665e-020)

C_{nr} = + (0) + M* (0) + α.*(-1.3332e-03)
+ (α.*M).* (6.6899e-04)+ (M.^2).* (-1.0842e+00) + (α.^2).* (1.6434e-03)
+ ((α.*M.^2).^2).* (-4.4258e-06) + (((α.^2).*M).^2).*(1.2017e-07) + ((α.*M).^2).*(1.0819e-05)
+ (((α.^2).* M.^2).^2).*(-2.8899e-09) + (M.^3).*(0) + (α.^3).*(-5.8118e-04)
+ (M.^4).*(2.7379e-01) + (α.^4).*(6.7994e-05) + (M.^5).*(-5.2435e-02) + (α.^5).* (-2.5848e-06)

Hypersonic

$C_{n\beta}$ = + (0) + α.* (6.9980e-04) + M.*(5.9115e-02) + (α.*M).*(-7.5250e-05) + ((α).^2).*(2.5160e-04)
+ ((M).^2).*(-1.4824e-02) + ((α.*M).^2).*(-2.1924e-07) + ((α).^3).*(-1.0777e-04) + ((M).^3).*(1.2692e-03)
+ ((α.*M).^3).* (1.0707e-08) + ((α).^4).*(9.4989e-06) + ((M).^4).*(-4.7098e-05) + ((α.*M).^4).*(-5.5472e-011)
+ ((α).^5).* (-2.5953e-07) + ((M).^5).*(6.4284e-07) + ((α.*M).^5).* (8.5863e-014)

$C_{n-\delta a}$ = + 2.10E-04 + α.*(1.83E-05) - M.*(3.56E-05) - δ_a.*(1.30E-05) - ((α.*M).* δ_a).*(8.93E-08)
- (α.^2).*(6.39E-07) + (M.^2).*(8.16E-07) + (δ_a.^2).*(1.97E-06) + (((α.*M).* δ_a).^2).*(1.41E-11)

$C_{n-\delta e}$ = -($C_{n-\delta a}$)

$C_{n-\delta r}$ = + 2.85E-18 - α.*(3.59E-19) - M.*(1.26E-19) - δ_r.*(5.28E-04)
+ (α.*δ_r).*(1.39E-05)+ (α.*M).*(1.57E-20) + (M.* δ_r).*(1.65E-05) - ((v.*M).* δ_r).*(3.13E-07)

C_{np} = + 3.68E-01 - M.*(9.79E-02) + α.*(7.61E-16) + (M.^2).*(1.24E-02)
- (α.^2).*(4.64E-16) - (M.^3).(8.05E-04) + (α.^3).*(1.01E-16) + (M.^4).(2.57E-05)
- (α.^4).*(9.18E-18) - (M.^5).*(3.20E-07) + (α.^5).*(2.96E-19)

C_{nr} = - 2.41E+00 + M.*(5.96E-01) - α.*(2.74E-03) + (α.*M).*(2.09E-04)
- (M.^2).*(7.57E-02) + (α.^2).*(1.15E-03) - ((α.*M).^2).*(6.53E-08) + (M.^3).*(4.90E-03)
- (α.^3).*(3.87E-04) - (M.^4).*(1.57E-04) + (α.^4).*(3.60E-05) + (M.^5).*(1.96E-06)
- (α.^5).*(1.18E-06)

V. Curve Fitting Procedure

Multi-variable curve fitting is a very challenging task. Acquiring an accurate curve to match a set of data can be a very time consuming process. Because of this, interpolation or extrapolation are more popular methods for implementing aerodynamic models. In this simulation, for the specific reason stated before, analytical expressions are preferred. The following Figures 2 through 24 evaluate the fit against the observed data points from the look-up tables.

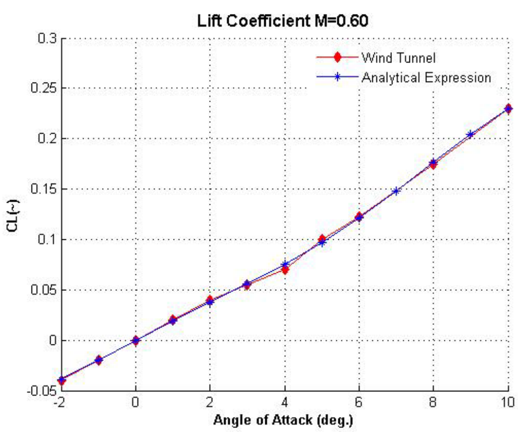

Figure 2: Lift Coefficient C_L (M=0.60)

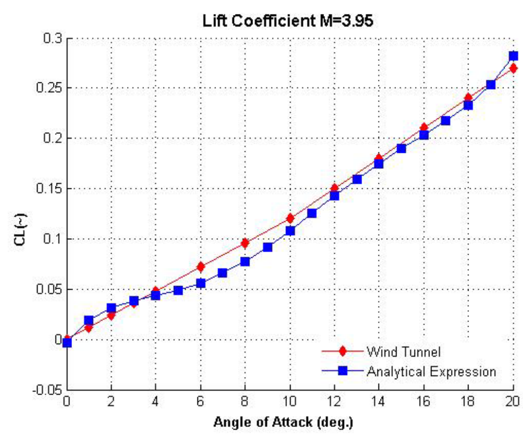

Figure 3: Lift Coefficient C_L (M=3.95)

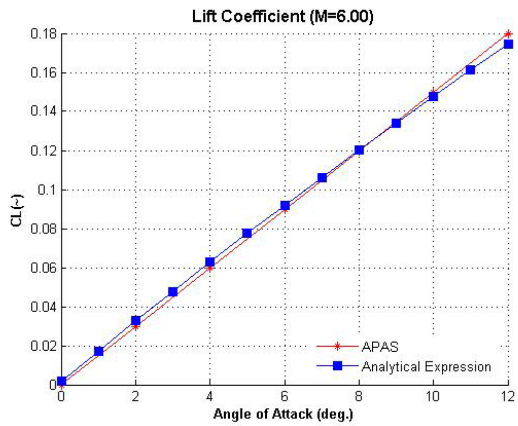

Figure 4: Lift Coefficient C_L (M=4.63)

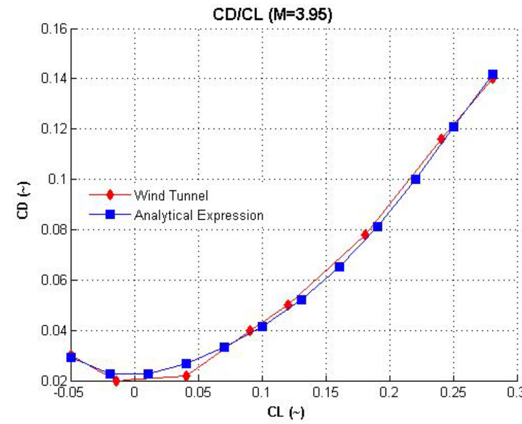

Figure 7: D/L (M=3.95)

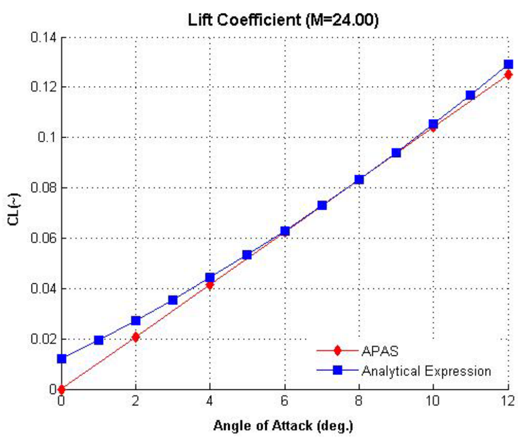

Figure 5: Lift Coefficient C_L (M=24.00)

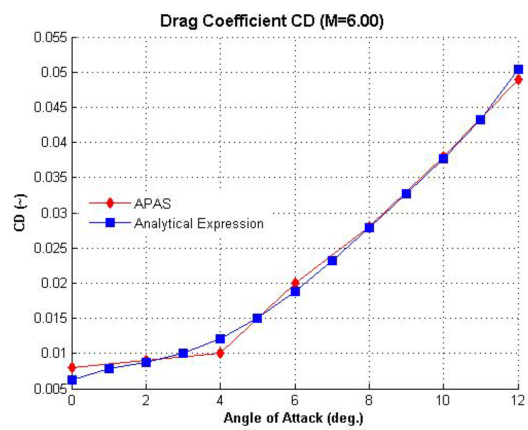

Figure 8: Drag Coefficient C_D (M=6.00)

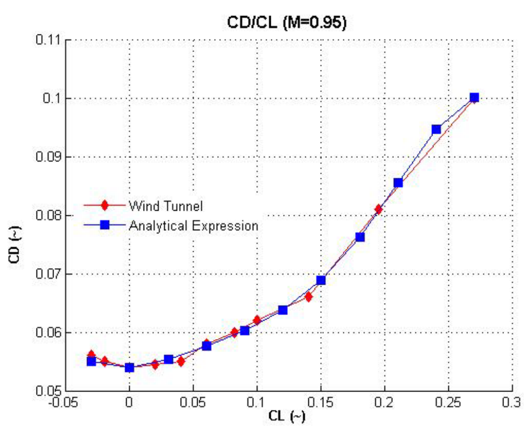

Figure 6: D/L Polar (M=0.95)

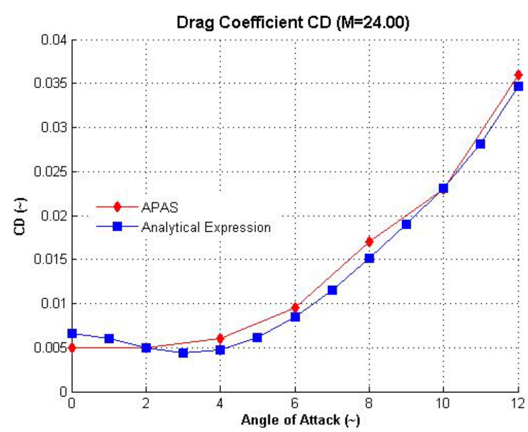

Figure 9: Drag Coefficient C_D (M=24.00)

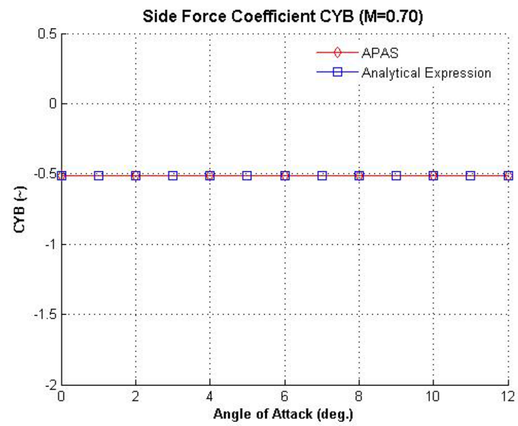

Figure 10: Side Force Coefficient $C_{Y\beta}$ (M=0.70)

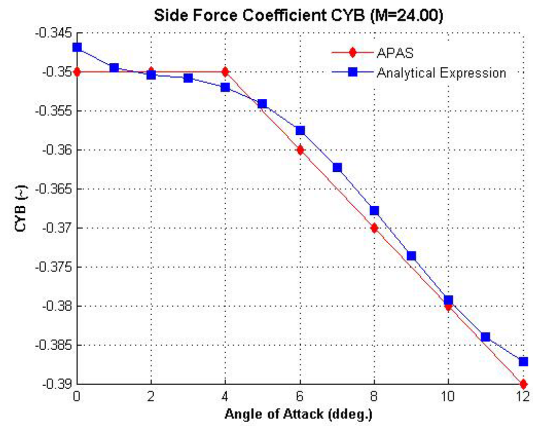

Figure 13: Side Force Coefficient $C_{Y\beta}$ (M=24.0)

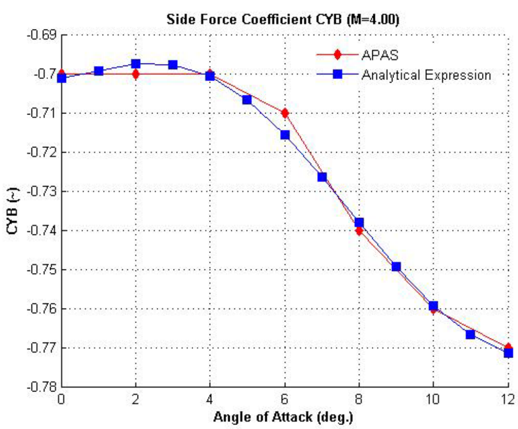

Figure 11: Side Force Coefficient $C_{Y\beta}$ (M=4.00)

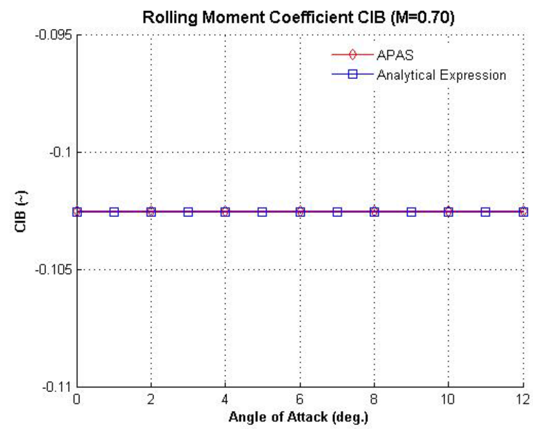

Figure 14: Rolling Moment Coefficient $C_{l\beta}$ (M=0.70)

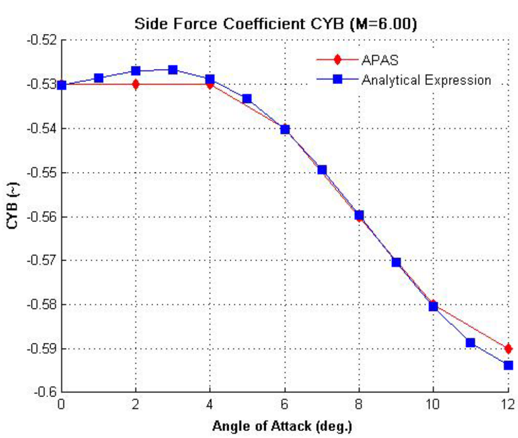

Figure 12: Side Force Coefficient $C_{Y\beta}$ (M=6.00)

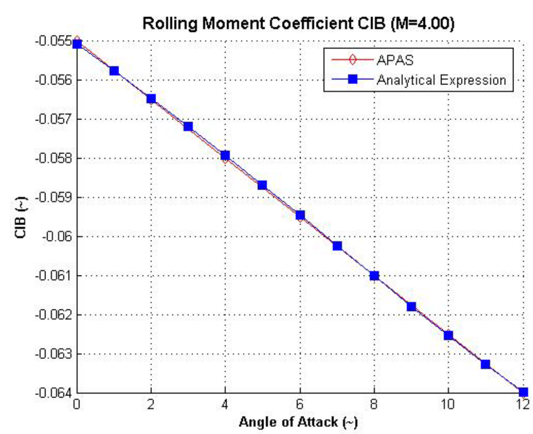

Figure 15: Rolling Moment Coefficient $C_{l\beta}$ (M=4.00)

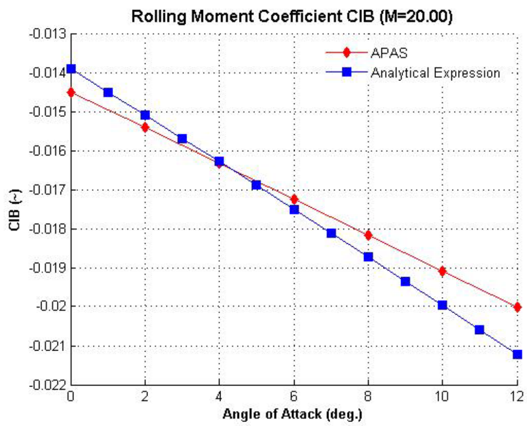

Figure 16: Rolling Moment Coefficient $C_{l\beta}$ (M=20.00)

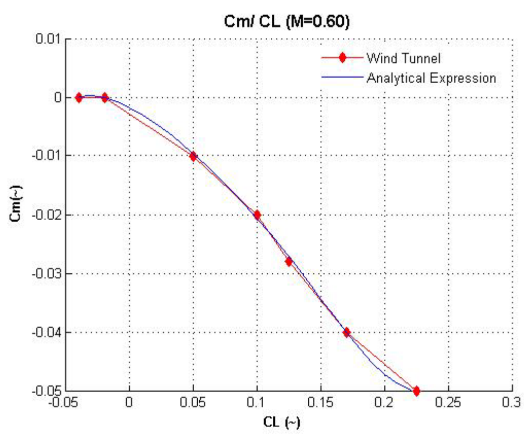

Figure 17: C_m/C_L (M=0.60)

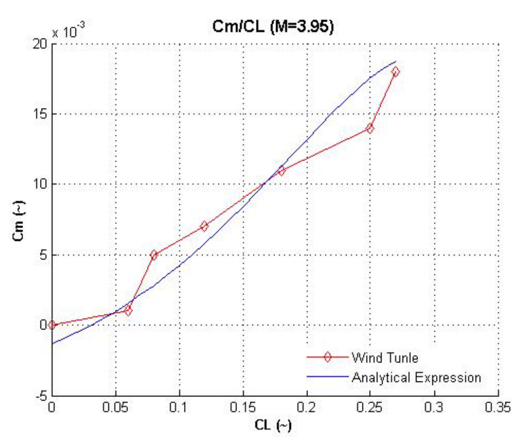

Figure 18: C_m/C_L (M=3.99)

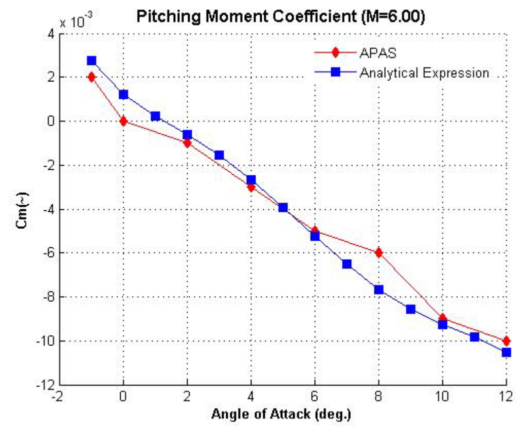

Figure 19: Pitching Moment Coefficient C_m (M=6.00)

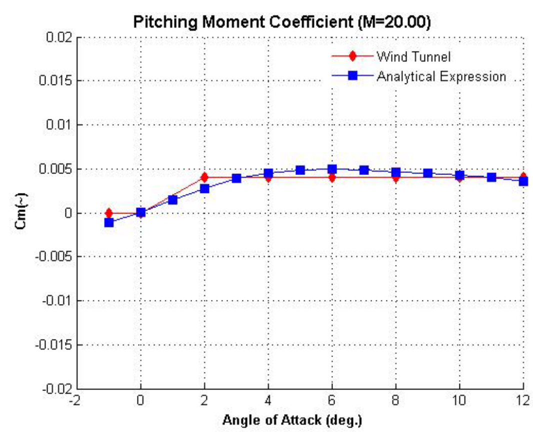

Figure 20: Pitching Moment Coefficient C_m (M=20.00)

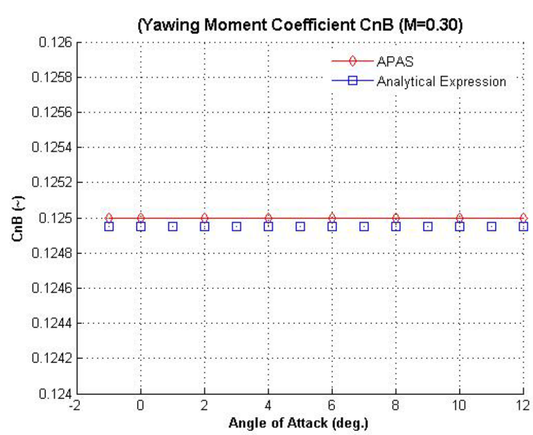

Figure 21: Yawing Moment Coefficient $C_{n\beta}$ (M=0.30)

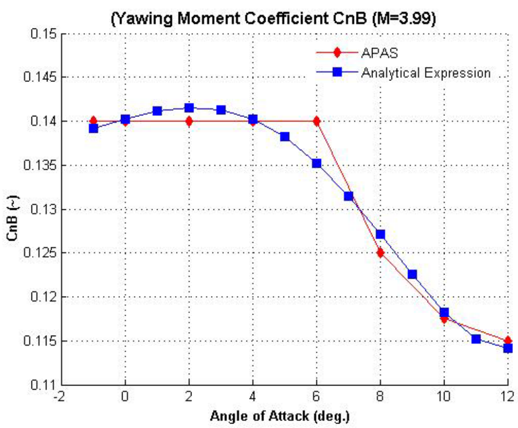

Figure 22: Yawing Moment Coefficient $C_{n\beta}$ (M=3.99)

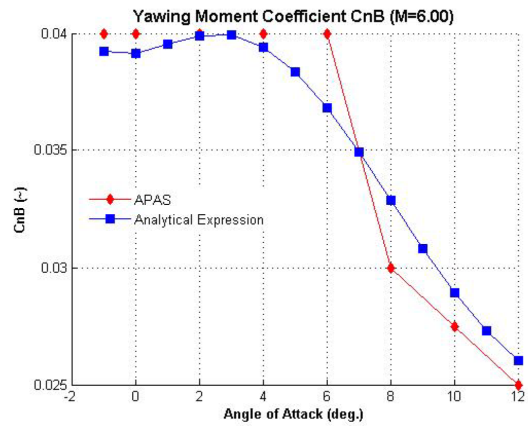

Figure 23: Yawing Moment Coefficient $C_{n\beta}$ (M=6.00)

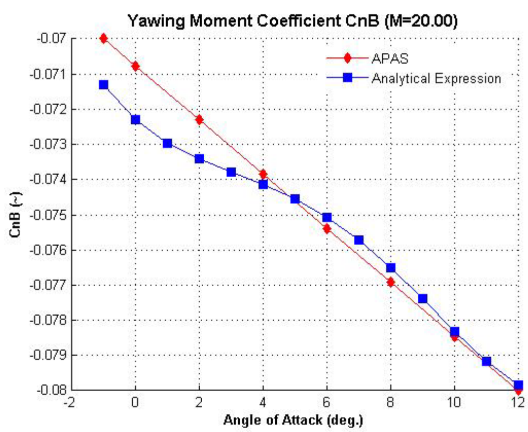

Figure 24: Yawing Moment Coefficient $C_{n\beta}$ (M=20.00)

VI. Comparison between Wind Tunnel Test Results and CFD Codes

Figures 25 through 31 show the comparison between the CFD codes generated results (APAS and STARS) and the equivalent wind tunnel data. Figure 1 shows the air vehicle configuration, which has a double delta wing planform. A typical variation of C_L with angle of attack has the following characteristics: the lift slope is small however, the lift continues to increase up to large values of angle of attack, and the stalling angle of attack is relatively high for subsonic and supersonic speeds. The stalling angle of attack is relatively smaller for hypersonic speeds. The following comparisons demonstrate that the wind tunnel data matches our expectation but the APAS and STARS results are not quiet satisfactory. In fact, because of the low lift curve slope, the $(L/D)_{max}$ is always less than 2.7 for supersonic and hypersonic speeds, as the wind tunnel results demonstrate. Figures 30 and 31 show that the CFD codes $(L/D)_{max}$ are much higher than expected. This is especially seen at M=6.00 where the STARS results is obviously incorrect. The APAS code gives reasonable results for the longitudinal aerodynamic coefficients for supersonic and for hypersonic flight conditions. The APAS results are not so good at subsonic speeds, especially at low angles of attack. The STARS code generated drag coefficient (C_D) is two times lower than the APAS results and three times lower than the wind tunnel results.

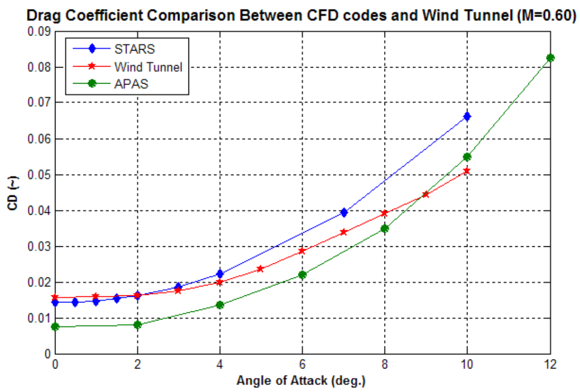

Figure 25: Wind Tunnel and CFD Codes Comparison
(CD @ M=0.60)

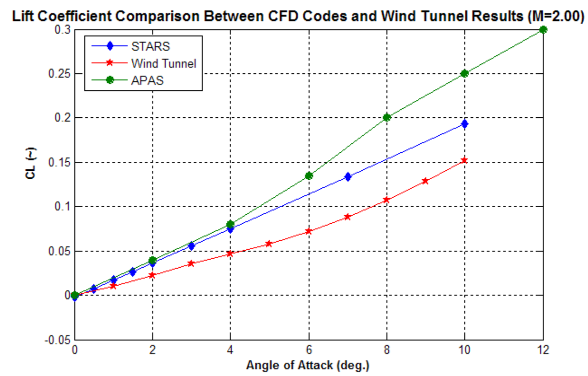

Figure 28: Wind Tunnel and CFD Codes Comparison
(CL @ M=2.00)

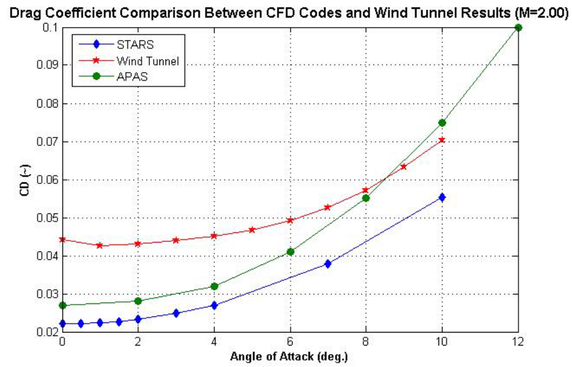

Figure 26: Wind Tunnel and CFD Codes Comparison
(CD @ M=2.00)

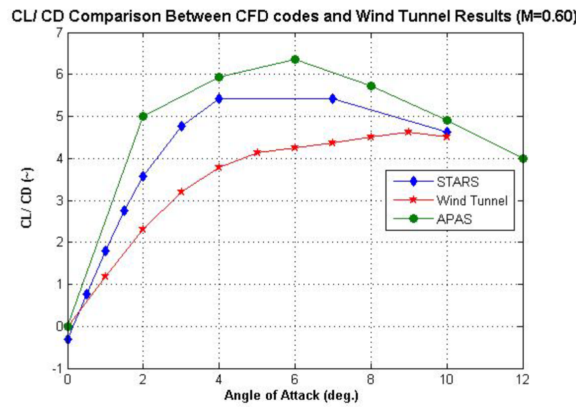

Figure 29: Wind Tunnel and CFD Codes Comparison
(CL/ CD @ M=0.60)

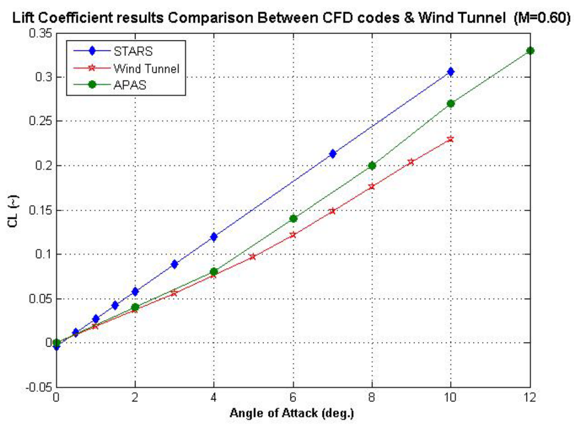

Figure 27: Wind Tunnel and CFD Codes Comparison
(CL @ M=0.60)

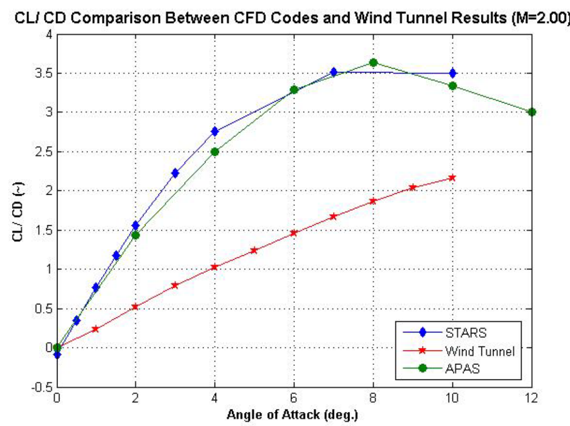

Figure 30: Wind Tunnel and CFD Codes Comparison
(CL/ CD @ M=2.00)

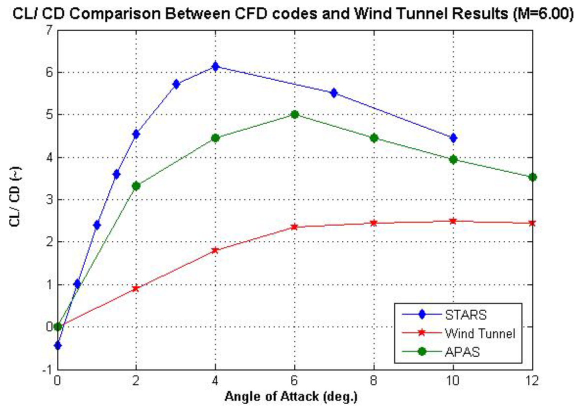

Figure 31: Wind Tunnel and CFD Codes Comparison (CL/ CD @ M=6.00)

VII. Engine Model

In order to operate through all Mach regimes, a combined-cycle propulsion system has been developed for the GHV. This engine is a combination of a hypothetical turbojet, ramjet, and rocket motor. Turbojets are particularly suited for the low-speed portions of the mission and have adequate performance up to Mach 3.0. These engine designs tend to operate with low overall pressure ratios and low rotor speeds at takeoff. Ramjets have no rotor machinery and only start to operate efficiently at speeds above Mach 2.0. In a ramjet the compression through the shock waves performs the same function as the compressor in turbojets, and this effect is substantial from M=2.00. The internal flow of the traditional ramjet engine is subsonic. Ramjet engines can be used to reach speeds up to Mach 6.0. This combined-cycle model is designed for a speed range from M=2.00 to M=4.00. For speeds above M=4.00 up to M=24.00 a rocket engine cycle is used. The engine deck generates a maximum of 330,000 lb thrust at 100% PLA. In this study the specific impulse I_{SP} was used instead of the exhaust velocity for the calculation of the thrust. I_{SP} is defined as the ratio of thrust to W_{prop}.

VIII. Flight Profile

This hypersonic vehicle operates within a fairly narrow range of dynamic pressures. If q_0 is too large, the forces and the drag on the air vehicle can be unnecessary high. On the other hand, if q_0 is too small then the wing area required for sustained flight may become excessively large. A high dynamic pressure is desirable for the best performance of the propulsion system. The flight trajectory is designed within a narrow range of q_0 of from 500.00 to 2000.00 psf (see Figure 32). The stagnation temperature experienced during hypersonic flight requires materials highly resistant to high temperatures for long periods of time. These are two other important factors in designing the flight trajectory considered within this research.

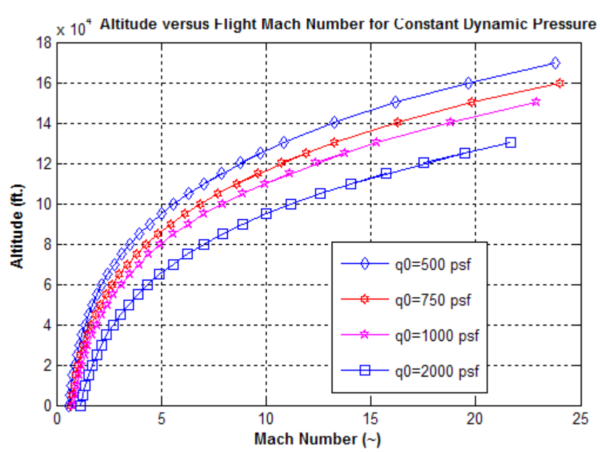

Figure 32: Altitude versus Flight Mach Number for a Constant Dynamic Pressure

Airbreathing engines generate thrust in direct proportion to the mass flow rate they are able to capture from the atmosphere. This shows the importance of trajectory selection for hypersonic air vehicles. Considering the air mass flow rate formula:

$$\rho_0 V_0 = \frac{2q_0}{V_0} = \frac{2q_0}{M_0\, a_0}$$

where a_0 barely changes over the flight altitudes. This means the air mass flow rate varies inversely with the Mach number along a constant dynamic pressure trajectory [4]. This fact adds more complexity to the hypersonic airbreathing engine design. As the air vehicle flies faster at a constant dynamic pressure, the available free stream mass flow rate per unit area reduces (see Figure 33).

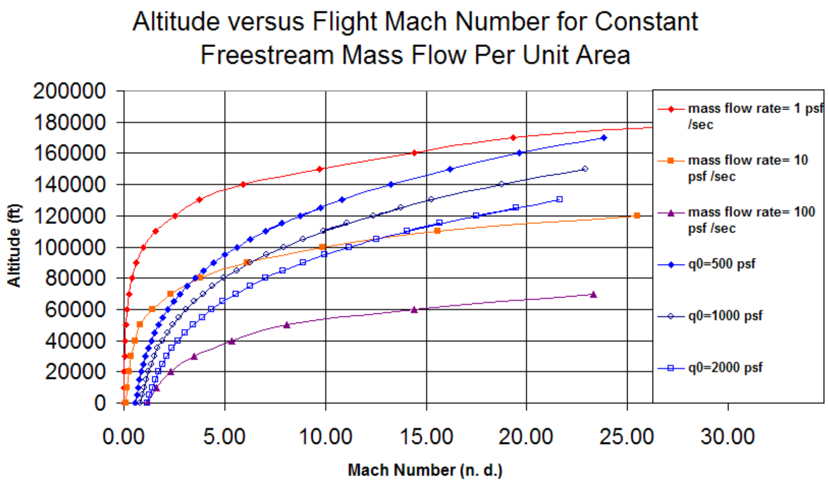

Figure 33: Altitude versus Flight Mach Number for Constant Free stream Mass Flow per Unit Area

IX. Flight Simulation

Using the previously discussed equations of motion, the simulation of the aerodynamic and propulsion forces and moments was accomplished. The simulation was implemented in visual Fortran. It was also implemented in MATLAB. The steady-state flight conditions are determined by solving the nonlinear state equations for the state and control vectors with constraints according to the flight condition(s).

X. Summary and Conclusions

This paper covers the development of a reliable aerodynamic database using three different resources. The six degrees of freedom simulation of a generic hypersonic vehicle (GHV) is implemented using this new aerodynamic model. The model and simulation were developed to support NASA and Air Force conceptual design studies of hypersonic vehicles with multiple cycle engines. The models were implemented in a combination of MATLAB and visual Fortran coded subroutines. The simulation includes both air breathing and rocket propulsion models. This work was partially supported under a NASA grant.

References

1. John D. Shaughnessy, S. Zane Pinckney, John D. McMinn, Christopher I. Cruz, and Marie-Louise Kelley, “Hypersonic Vehicle Simulation Model, Winged-Cone Configuration,” NASA Technical Memorandum 102610, NASA Langley, 1991.
2. Sang Bum Choi, “Investigation of the aerodynamic characteristics of the Generic Hypersonic Vehicle, Winged-Cone Configuration, by STARS CFD codes,” MFDCLAB, Los Angeles, California, 2005.
3. W. Pelham Phillips, Gregory J. Brauckmann, John R. Mico and William C. Woods, “Experimental Investigation of the Aerodynamic Characteristics for a Winged-Cone Concept,” NASA Langley Research Center.

4. William H. Heiser, David T. Pratt, “Hypersonic Airbreathing Propulsion,” AIAA Educational Series, 1994.
5. W. Pelham Philips, Gregory J. Brauckmann, and William C. Woods, “Experimental Investigation of the Aerodynamic Characteristics for a Winged-Cone Concept,” AIAA 87-49098.
6. Charles E. Dole, James E. Lewis, “Flight Theory and Aerodynamics, Second Edition,” 2000.
7. Banu N. Pamadi, “Performance, Stability, Dynamics, and Control of the Airplane,” AIAA Educational Series, 1998.
8. Peter H. Zipfel, “Modeling and Simulation of Aerospace Vehicle Dynamics,” AIAA Educational series, 2000.
9. Frank L. Lewis and Brian L. Stevens, “Aircraft Control and Simulation,” Wiley, 1992.
10. Jan Roskam, “Airplane Flight Dynamics and Automatic Flight Control part I,” DAR Corporation, 1997.
8. “NASA Hypersonic Research at the Edge of Space,” http://www.hq.nasa.gov/office/pao/History/x15/cover.html.
9. E. T. Curran and S. N. B. Murthy, “Scramjet Propulsion,” Department of the Air Force (Editor), Purdue University.